

## REPORT DOCUMENTATION PAGE

Form Approved  
OMB No. 0704-0188

Public reporting burden for this collection of information is estimated to average 1 hour per response, including the time for reviewing instructions, searching existing data sources, gathering and maintaining the data needed, and completing and reviewing the collection of information. Send comments regarding this burden estimate or any other aspect of this collection of information, including suggestions for reducing this burden, to Washington Headquarters Services, Directorate for Information Operations and Reports, 1215 Jefferson Davis Highway, Suite 1204, Arlington, VA 22202-4302, and to the Office of Management and Budget, Paperwork Reduction Project (0704-0188), Washington, DC 20503.

1. AGENCY USE ONLY (Leave blank)		2. REPORT DATE 10-17-95	3. REPORT TYPE AND DATES COVERED	
4. TITLE AND SUBTITLE Cooling Characteristics and SHape Memory Effects of R-Phase NiTi Alloys			5. FUNDING NUMBERS  DAAL03-91-G-0245	
6. AUTHOR(S) Y. Q. Liu, Z. J. Pu, K. H. Wu			8. PERFORMING ORGANIZATION REPORT NUMBER	
7. PERFORMING ORGANIZATION NAME(S) AND ADDRESS(ES) Florida International University University Park Miami, FL 33199			10. SPONSORING / MONITORING AGENCY REPORT NUMBER  ARO 29150.12-MS - SAH	
9. SPONSORING / MONITORING AGENCY NAME(S) AND ADDRESS(ES) U.S. Army Research Office P. O. Box 12211 Research Triangle Park, NC 27709-2211				
11. SUPPLEMENTARY NOTES The views, opinions and/or findings contained in this report are those of the author(s) and should not be construed as an official Department of the Army position, policy, or decision, unless so designated by other documentation.				
12a. DISTRIBUTION / AVAILABILITY STATEMENT  Approved for public release; distribution unlimited.			12b. DISTRIBUTION CODE	
13. ABSTRACT (Maximum 200 words)  Numerical and experimental studies are carried out to characterize the response time and shape memory effects of an R-Phase NiTi alloy. The results of the numerical analysis indicate that the response speed of the R-Phase alloy can be four to six times faster than martensite NiTi alloys. The experimental results demonstrate that the R-Phase NiTi alloy is a superior smart material to the martensite-based NiTi alloy when response time is indeed a requirement.				
DTIC QUALITY INSPECTED 1				
14. SUBJECT TERMS			15. NUMBER OF PAGES 6	
			16. PRICE CODE	
17. SECURITY CLASSIFICATION OF REPORT UNCLASSIFIED		18. SECURITY CLASSIFICATION OF THIS PAGE UNCLASSIFIED	19. SECURITY CLASSIFICATION OF ABSTRACT UNCLASSIFIED	20. LIMITATION OF ABSTRACT UL

# DISCLAIMER NOTICE



**THIS DOCUMENT IS BEST  
QUALITY AVAILABLE. THE  
COPY FURNISHED TO DTIC  
CONTAINED A SIGNIFICANT  
NUMBER OF PAGES WHICH DO  
NOT REPRODUCE LEGIBLY.**

# **SHAPE MEMORY MATERIALS '94**

## **PROCEEDINGS OF THE INTERNATIONAL SYMPOSIUM ON SHAPE MEMORY MATERIALS**

**September 25-28**

**Beijing, China**

**Edited by CHU Youyi  
TU Hailing**

19960209 125



**INTERNATIONAL ACADEMIC PUBLISHERS**

## COOLING CHARACTERISTICS AND SHAPE MEMORY EFFECTS OF R-PHASE NiTi ALLOYS

Y. Q. Liu, Z. J. Pu, and K. H. Wu  
(Florida International University, Miami, FL 33199, USA)

### ABSTRACT

Numerical and experimental studies are carried out to characterize the response time and shape memory effects of an R-phase NiTi alloy. The results of the numerical analysis indicate that the response speed of the R-phase alloy can be four to six times faster than the martensite NiTi alloys. The experimental results demonstrate that the R-phase NiTi alloy has almost the same shape memory effect as the martensite NiTi alloy. It can be concluded that the R-phase NiTi alloy is a superior smart material to the martensite based NiTi alloy when fast response time is indeed a requirement.

### INTRODUCTION

Shape memory alloys (SMAs) have been recognized as important intelligent materials due to their accurate temperature response, energetic recovery force, miniature size, and good durability<sup>1-3,6</sup>. Having many advantages, they have been used extensively in smart structures for active shape controlling, smart actuators, and sensors. The major problem of the martensite based NiTi alloy as a smart material is its long response time due to its slow cooling rate, which is an intrinsic nature of the material. As a consequence, shape memory alloys have been regarded as low-frequency response materials. However, based on this study, it was found that the R-phase NiTi alloy possesses many remarkable features, such as lower hysteresis width (1.5°C)<sup>4</sup>, lower enthalpy change during the R-phase  $\rightleftharpoons$  austenite transformation ( $\Delta H=5$  J/g), and excellent fatigue resistance<sup>5</sup>. Inasmuch, the R-phase alloys can respond with a much faster speed than the ordinary martensite based NiTi alloys. In this paper, theoretical heat transfer analysis and experimental tests were performed to evaluate the response characteristics and the shape memory effect of the R-phase NiTi alloy.

### THE HEAT TRANSFER MODEL AND THE EXPERIMENTAL PROCEDURES

The heat transfer problem is illustrated by a cylindrically shaped memory wire. The SMA wire is modeled as a long cylinder with uniform internal heat generation due to resistance heating. A number of assumptions can be made to simplify the analysis without compromising the quantitative nature of the result. First, the wire is assumed to be very long in comparison with the diameter such that temperature variations in the longitudinal direction are negligible. Second, the wire is assumed to have uniform temperature over the cross section. By incorporating these assumptions, the heat transfer equation is reduced to a simple one-dimensional axisymmetric problem shown below:

$$\frac{dq}{dt} = \frac{dE}{dt}, \quad (1)$$

where  $dq/dt$  is the heat transfer rate to or from the SMA wire, and  $dE/dt$  is the rate of the energy stored in the SMA wire.

Prior to initiation of the martensite-to-austenite transformation, the heat input simply changes the internal energy of the SMA. The energy change corresponding to a prescribed temperature change is given by: where  $C_p$  is the constant-pressure specific heat of the SMA wire,  $m$  is the mass of the wire, and  $T$  is the temperature. In contrast, when the martensite-to-austenite solid transformation begins, the amount of input energy required to increase the SMA temperature must include the latent heat of transformation as shown below:

$$\frac{dE}{dt} = mC_p \frac{dT}{dt}, \quad (2)$$

$$\frac{dE}{dt} = mC_p \frac{dT}{dt} - m\Delta H \frac{df}{dt}, \quad (3)$$

where  $f$  is the martensite fraction and  $\Delta H$  is the latent heat (enthalpy change) of the transformation. The amount of energy required during the solid-solid phase transformation is assumed to vary linearly with the martensite fraction,  $f$ .<sup>6</sup> The martensite volume fraction,  $f$ , does not change from 0 - 100 % at a single transformation temperature, but rather changes continuously throughout the transition region. A simple cosine function for the martensite volume fraction,  $f$ , as a function of temperature has been proposed by Liang and Rogers<sup>6</sup> and is used in this investigation. For the martensite to austenite transformation, the martensite volume fraction is given by:

$$f = \frac{1}{2} \left[ 1 + \cos \pi \left( \frac{T - A_s}{A_f - A_s} \right) \right], \quad (4)$$

while during the transformation from austenite to martensite, it is given by:

$$f = \frac{1}{2} \left[ 1 + \cos \pi \left( \frac{T - M_f}{M_s - M_f} \right) \right]. \quad (5)$$

Based on Eqs. (4) and (5), the expression for  $dE/dt$  for the martensite to austenite transformation reduces to:

$$\frac{dE}{dt} = mC_p \frac{dT}{dt} + \frac{1}{2} \pi m \Delta H (A_f - A_s) \left[ \sin \pi \left( \frac{T - A_f}{A_f - A_s} \right) \right] \frac{dT}{dt}, \quad (6)$$

and the  $dE/dt$  for the austenite to martensite transformation reduces to

$$\frac{dE}{dT} = mC_p \frac{dT}{dt} + \frac{1}{2} \pi m \Delta H (M_s - M_f) \left[ \sin \pi \left( \frac{T - M_f}{M_s - M_f} \right) \right] \frac{dT}{dt}. \quad (7)$$

The  $dq/dt$  term in Eq. (1) is a function of the environmental condition of the SMA wire. In this paper, the wire was assumed to have free convection cooling. The heating of the wire is assumed to be induced by resistance heating. Thus,  $dq/dt$  can be described as follows:

$$\frac{dq}{dt} = I^2 R - hA(T - T_{env}) \quad (8)$$

$$\frac{dq}{dt} = -hA(T - T_{env}). \quad (9)$$

Equations (8) and (9) correspond to the heat transfer rate for heating and cooling, respectively, where  $A$  is the surface area of the wire,  $T_{env}$  is the environment temperature, and  $h$  is the convection coefficient.

The composition of the alloy studied is Ti-50.6 at% Ni. Two types of heat treatment procedures were used: one was to anneal the cold deformed sample at 300°C for 100 hours, and the other was to heat treat the sample at 850°C and then quench it in water. The phase transformation behavior was characterized using a Differential Scanning Calorimeter (DSC). An X-ray diffractometer was used to characterize the crystal structure of the transformation products. Mechanical tests were conducted to: i) quantify the strain recovery behavior during the phase transformation process as a function of pre-strain, and ii) measure the recovery stress as a function of pre-strain. The tensile specimens with a gage length of 24.5 mm and diameter of 3 mm were machined from bar stock using a grinding method. The tests were carried out on a closed-loop servo-hydraulic Instron model 1331 cycle tester in

a water environment.

## RESULTS AND DISCUSSION

Figures 1a and 1b show the cycle time of SMAs as a function of  $\Delta H$  and hysteresis width,  $\Delta T$ . In this calculation, it was assumed that  $A_s=348$  K,  $A_f=363$  K,  $M_s=363-\Delta T$ , and  $M_f=M_s-30$ . The other parameters, such as constant pressure specific heat,  $C_p$ , the specific resistance,  $\rho_e$ , density,  $\rho_w$ , and convection coefficient,  $h$ , were assumed to be 250 J/kg-K, 0.115  $\Omega$ -cm, 5.97 kg/cm<sup>3</sup>, and 22 w/cm-K, respectively. Figures 1a and 1b correspond to the wires with 0.1 mm and 1.0 mm diameters, respectively. It clearly shows that the cycle time increases with increasing  $\Delta H$  and  $\Delta T$ . For the R-phase alloy, it was determined that  $\Delta H=5-7$  kJ/kg, and  $\Delta T=2-5$  K, while the corresponding values for the martensite shape memory alloys were  $\Delta=30$  KJ/kg and  $\Delta T=25-40$  K. The martensite SMA and R-phase SMA are marked clearly in Fig. 1. According to the results, it is apparent that the cycle time of R-phase SMA is only 1/4 to 1/6 that of the martensite SMAs.

Figure 2 shows the thermal cycle process of typical martensite SMAs and R-phase SMA alloys. These temperature profiles consist of four distinct parts. Part 1 represents the heating prior the martensite-to-austenite transformation. As is evident in the figure, the heating portion takes very minimal time and is primarily a function of applied current. Part 2 illustrates the heating during the transformation process. Although the current remains unchanged for part 1, it is obvious that the heating of part 2 is slower than that of part 1 due to the endothermic nature of the transformation. The cooling portion prior to the martensite transformation that is depicted in part 3 and part 4 demonstrates the cooling process during the austenite-to-martensite transformation. The cooling rate of this part is the slowest of the entire cycle due to the exothermic process of the martensite transformation. When comparing the cooling times for each part, it appears that the heating time takes approximately only 1/10 of the total cycle time and 90% of the time is spent on cooling the sample in ordinary martensite alloys. The results clearly suggest that the most important step toward reducing the cycle time is to reduce the cooling time. In the cooling cycle, the time of part 3 pertains to the hysteresis width of the material and the time of part 4 is directly related to the exothermic heat of the transformation. Therefore, it is apparent that narrowing down the hysteresis width and decreasing the exothermic heat are effective ways to reduce the cycle time. This is clearly demonstrated in Figs. 2a and 2b. In the R-phase alloy, the time spent in part 3 is only 1/13 of that spent on martensite alloys because the R-phase alloy has a very narrow hysteresis width. In addition, the time spent in part 4 for the R-phase alloy is only 1/4 that of martensite alloys because the R-phase alloy has a very low  $\Delta H$ .

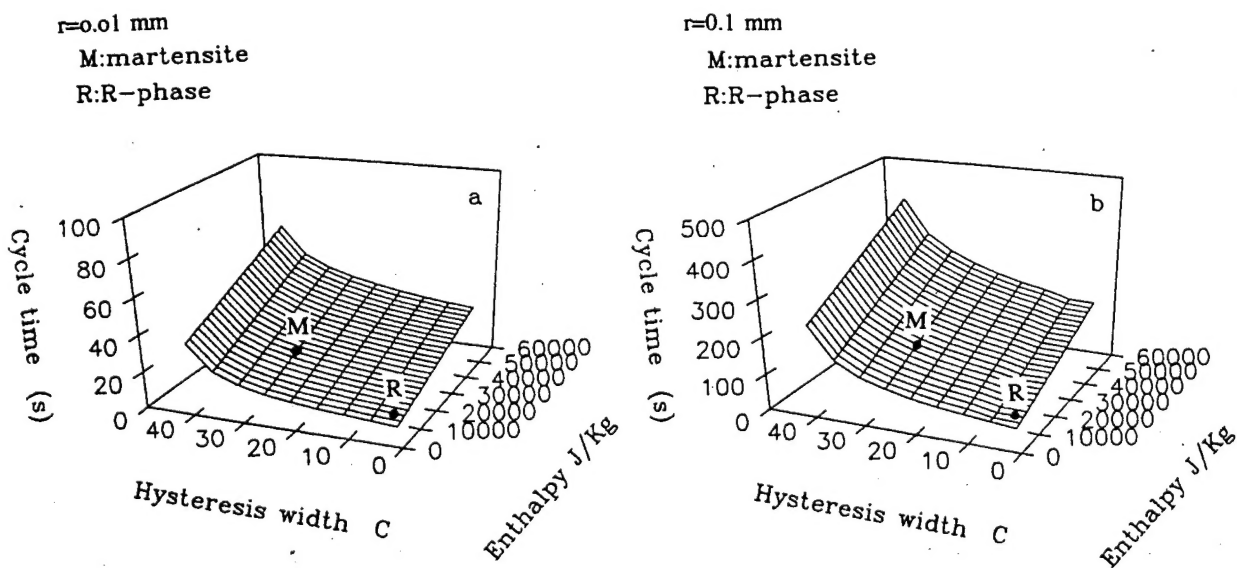


Figure 1. The cycle time of SMAs as a function of hysteresis width,  $\Delta$  transformation enthalpy change and wire diameters.

Figure 3 shows the DSC curves of various SMA samples. In this figure, one sample was annealed at 300°C for 100 hours and the other was heated at 850°C for 0.5 hours followed by water quenching. In order to achieve a fully R-phase sample, the alloy was annealed at 300°C for 300 hours and then quenched to 20°C in water. According

to the DSC curve, as shown in Fig. 3a, the transformation product appears to be R-phase.

Figure 4 shows the typical stress-strain curves of the fully R-phase sample at room temperature. The sample exhibits two plateaus. The first one begins at 0.15% strain and finishes at a strain value of 0.7%. The second one begins with a strain of 2% and finishes at 6.5%. Miyazaki and Otsuka proposed [7] that the first plateau associated with the rearrangement of the R-phase variates to a favorable one, and the second plateau corresponds to the stress-induced martensite transformation. Figure 5 shows the X-ray diffraction spectrums. The data shown in (a), (b), and (c) correspond to the 300°C annealing sample, the 850°C quenched sample, and the deformed sample ( $\epsilon=6\%$ ), respectively. It is evident from these figures that R-phase is the predominant phase and the martensite is a minor phase for the sample annealed at 300°C. Nearly 100% martensite was found after the specimen was water-quenched. After subjecting the sample to a 6.5% deformation, the martensite peak intensity is somewhat higher than that of the original sample. It is difficult to identify the existence of a stress induced martensite transformation in the second plateau, as proposed by other authors<sup>7</sup>. Further work is needed to characterize the mechanism of the second plateau.

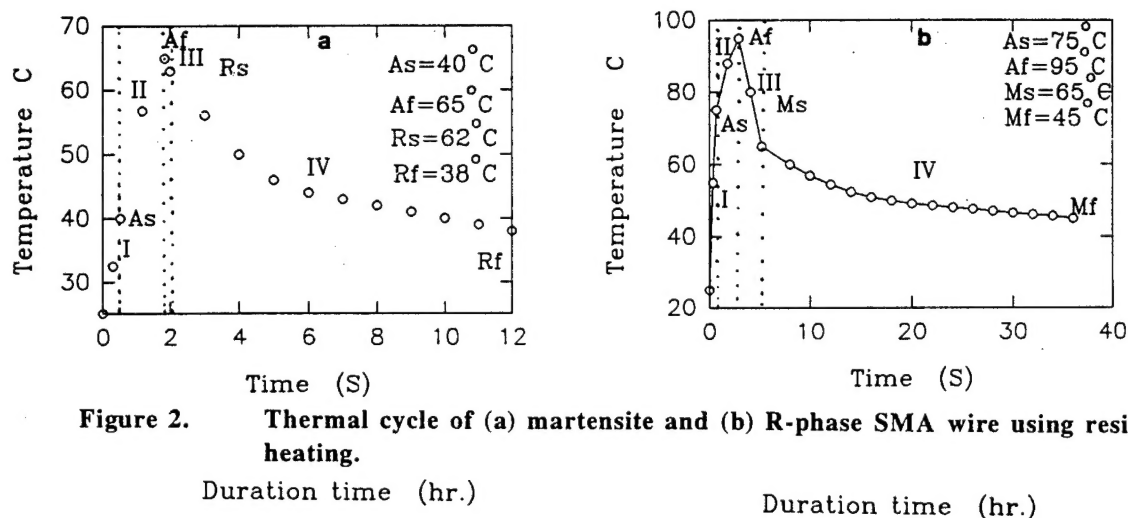


Figure 2. Thermal cycle of (a) martensite and (b) R-phase SMA wire using resistance heating.

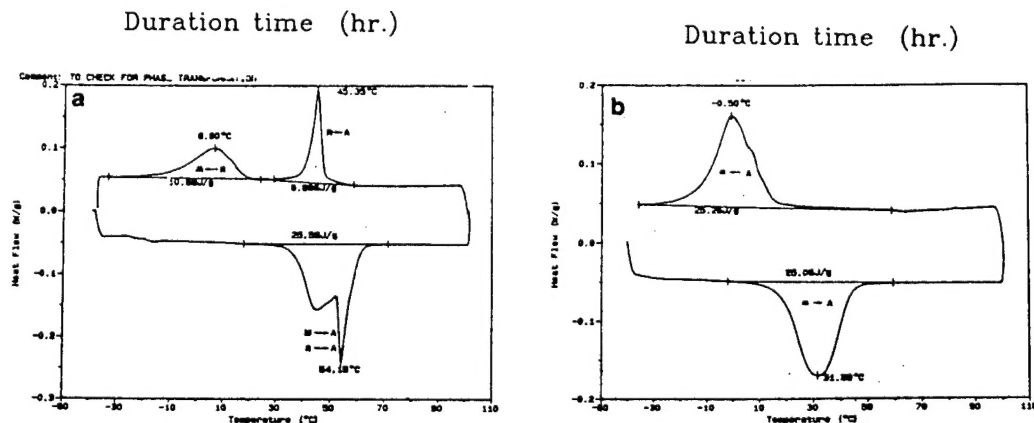


Figure 3. The DSC curves of (a) annealed sample at 300°C for 100 hours, and (b) quenched sample at 850°C for 0.5 hours.

Figure 6 shows the strain recovery process of the R-phase alloys. It can be clearly seen that the R-phase sample can recover as much as 7% of its strain after pre-deformation. This is almost the same magnitude as that of the martensite-based shape memory alloys. Figure 7 demonstrates the recovery stress of the samples. One sample was pre-deformed to 1% strain and another was pre-deformed to 6.5%, which corresponds to the finished points of the first and second plateaus, respectively. Based on Fig. 6, it becomes clear that the pre-strain does not play an important role in recovery stress. For example, the sample with 6.5% pre-strain has almost the same recovery stress as the sample with a pre-strain of only 1%. For the martensite-based shape memory alloys, the recovery stress strongly depends on the pre-strain. At present, it is not clear why the recovery stress of R-phase alloys is independent of pre-strain. In comparison with the martensite-based alloys, the R-phase NiTi alloys have similar high recovery stresses, because in the martensite-based shape memory alloys, a maximum recovery stress of 400 MPa was reported<sup>8</sup>, while 370 MPa was measured in the R-phase NiTi alloy. The ratio of Young's modulus of austenite to R-phase is 3.2, which is the same as that of austenite to martensite<sup>8</sup>.

The numerical analysis clearly demonstrates that the overall response time of R-phase alloys is only 1/4-1/6 of that of martensite-based NiTi alloys. On the other hand, the experimental results indicate that the R-phase NiTi alloy



has the same shape memory effect of the martensite NiTi alloy. Based on these two important facts, it can be concluded that R-phase alloy is a superior smart material to martensite-based NiTi alloy in high-frequency response applications. The R-phase NiTi alloys can respond 4-6 times faster than the martensite NiTi alloys.

## CONCLUSIONS

1. A numerical analysis indicates that 90% of the response time of an SMA wire is spent on cooling. Reducing the hysteresis width and  $\Delta H$  can significantly reduce the response time of the SMA material.
2. The response time of the R-phase NiTi alloy is only 1/4-1/6 that of the martensite-based NiTi alloy. As a result, for higher frequency smart material applications, the R-phase alloy is superior to the martensite-based NiTi alloy.
3. The shape memory effect of the R-phase NiTi alloy is almost the same as that of the martensite-based NiTi alloy.

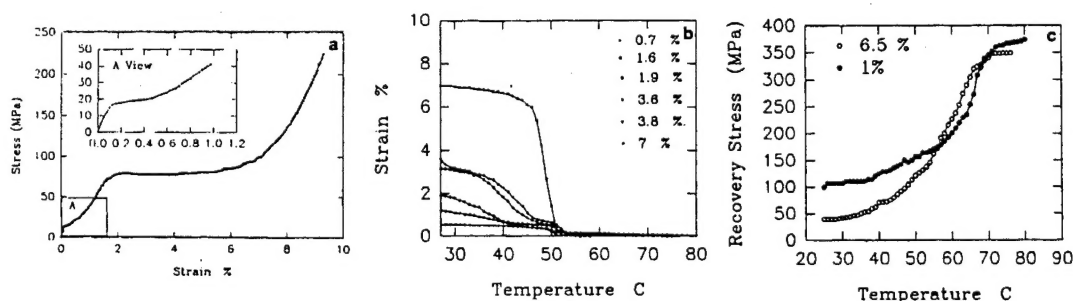


**Figure 4.** The stress-strain curve of the R-phase sample (a), and strain recovery process (b), and recovery stress of the R-phase samples (c).

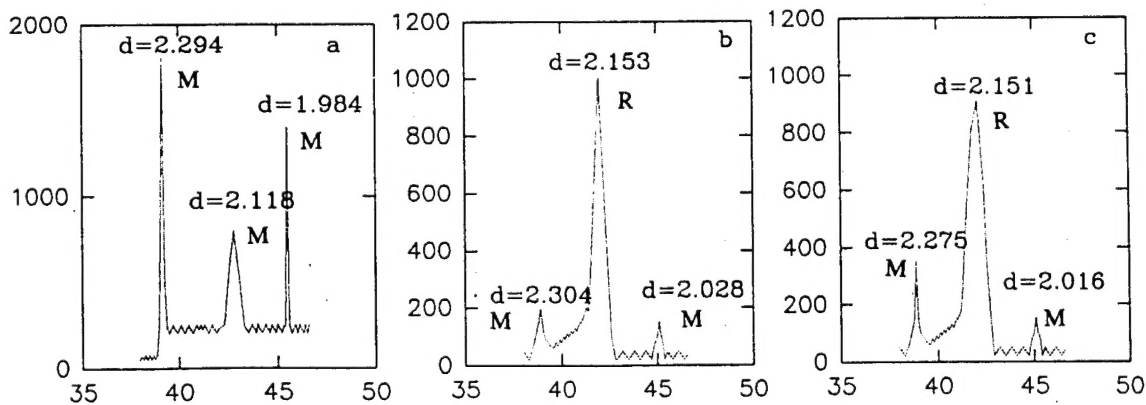


**Figure 5.** The X-ray diffraction spectrums of (a) the annealed sample, (b) the quenched sample, and (c) the annealed sample after 6% deformation.

## REFERENCES

1. B. J. Maclean, G. J. Patterson, and M. S. Misra, *J. Intell. Mater. and Struc.* V1(1990), p. 72.
2. J. J. Hollkamp, *J. Intell. Mater. and Struc.* V5(1994), p.49.
3. A. Craig and J. Rogers, *Acoust. Soc. Am.* 88(1990), p. 2803.
4. K. Otsuta, *Engineering of Shape Memory Alloy*, Butterworth, p. 36 (1990), Ed. by T. W. Duerig, K. N. Melton, D. Stockel, and C. M. Wayman.
5. Y. Suzuki and H. Tumara, *Engineering of Shape Memory Alloy*, Butterworth, p. 256 (1990), Ed. by T. W. Duerig, K. N. Melton, D. Stockel and C. M. Wayman.
6. C. Liang and C. A. Rogers, *J. Intell. Mater. and Struc.* V1(1990), p. 207.
7. S. Miyazaki and K. Otsuka, *Metall. Trans.* 17A(1986), P.53.
8. C. M. Jackson, H. J. Wagner, and R. J. Wasilewski, *NASA-SP-5110*, p. 9 (1972).